

## Enhanced photoresponse of a metal-oxide-semiconductor photodetector with silicon nanocrystals embedded in the oxide layer

Jia-Min Shieh, Yi-Fan Lai, Wei-Xin Ni, Hao-Chung Kuo, Chih-Yao Fang, Jung Y. Huang, and Ci-Ling Pan

Citation: [Applied Physics Letters](#) **90**, 051105 (2007); doi: 10.1063/1.2450653

View online: <http://dx.doi.org/10.1063/1.2450653>

View Table of Contents: <http://scitation.aip.org/content/aip/journal/apl/90/5?ver=pdfcov>

Published by the [AIP Publishing](#)

---

### Articles you may be interested in

[Effects of postgate dielectric treatment on germanium-based metal-oxide-semiconductor device by supercritical fluid technology](#)

Appl. Phys. Lett. **96**, 112902 (2010); 10.1063/1.3365177

[Near-infrared silicon quantum dots metal-oxide-semiconductor field-effect transistor photodetector](#)

Appl. Phys. Lett. **94**, 241108 (2009); 10.1063/1.3156806

[Superlinear photovoltaic effect in Si nanocrystals based metal-insulator-semiconductor devices](#)

Appl. Phys. Lett. **94**, 062108 (2009); 10.1063/1.3081410

[Subband gap photoresponse of nanocrystalline silicon in a metal-oxide-semiconductor device](#)

J. Appl. Phys. **104**, 074917 (2008); 10.1063/1.2999561

[Si avalanche photodetectors fabricated in standard complementary metal-oxide-semiconductor process](#)

Appl. Phys. Lett. **90**, 151118 (2007); 10.1063/1.2722028

---

The advertisement features a dark blue background with white and orange text. At the top left, it reads 'NEW! Asylum Research MFP-3D Infinity™ AFM' in large white letters, followed by 'Unmatched Performance, Versatility and Support' in orange. On the right, the 'OXFORD INSTRUMENTS' logo is shown in white, with the tagline 'The Business of Science®' below it. The central part of the ad contains four images with descriptive text: 1) A blue textured surface with the text 'Stunning high performance'. 2) A brown textured surface with the text 'Simpler than ever to GetStarted™'. 3) A yellow and brown patterned surface with the text 'Comprehensive tools for nanomechanics'. 4) A white and blue AFM instrument with the text 'Widest range of accessories for materials science and bioscience'. A small image of a multi-colored chip is also visible.

# Enhanced photoresponse of a metal-oxide-semiconductor photodetector with silicon nanocrystals embedded in the oxide layer

Jia-Min Shieh,<sup>a)</sup> Yi-Fan Lai, and Wei-Xin Ni

National Nano Device Laboratories, No. 26 Prosperity Road 1, Hsinchu, Taiwan 30078, Republic of China

Hao-Chung Kuo, Chih-Yao Fang, Jung Y. Huang, and Ci-Ling Pan

Department of Photonics and Institute of Electro-Optical Engineering, National Chiao Tung University, 1001 Ta Hsueh Road, Hsinchu, Taiwan 30010, Republic of China

(Received 24 October 2006; accepted 6 January 2007; published online 30 January 2007)

The authors report a two-terminal metal-oxide-semiconductor photodetector for which light is absorbed in a capping layer of silicon nanocrystals embedded in a mesoporous silica matrix on *p*-type silicon substrates. Operated at reverse bias, enhanced photoresponse from 300 to 700 nm was observed. The highest optoelectronic conversion efficiency is as high as 200%. The enhancements were explained by a transistorlike mechanism, in which the inversion layer acts as the emitter and trapped positive charges in the mesoporous dielectric layer assist carrier injection from the inversion layer to the contact, such that the primary photocurrent could be amplified. © 2007 American Institute of Physics. [DOI: 10.1063/1.2450653]

Photodetectors are essential optoelectronic devices<sup>1</sup> for a variety of applications, ranging from biomedicine<sup>2</sup> to optical storage.<sup>3</sup> Although bulk silicon (Si) has been widely used in the mainstream electronic chip technology, so far it fails for device applications in optoelectronics due to an indirect band gap of 1.1 eV. Nanoscaled engineered Si materials with size-dependent properties in electronic states,<sup>4</sup> however, are potential candidates for photonic devices. In particular, two kinds of Si-based nanostructured materials, namely, thin films of silicon nanocrystals<sup>5</sup> (nc-Si, 1–2 nm in characteristic size) and porous silicon,<sup>6,7</sup> were shown to be efficient for photodetection with spectral response from near infrared to the ultraviolet (UV).

Detection amplification in photodetectors is a concern and also gives another means to enhance the device sensitivity,<sup>8</sup> i.e., although the primary photoresponse may not be very high, the eventually measured photocurrent could be improved due to the device amplification function. The known detector solutions of this type are the avalanche photodiodes,<sup>9</sup> phototransistors,<sup>10</sup> photo-metal-oxide-semiconductor field-effect transistors,<sup>11</sup> etc.

In this letter, we report enhanced spectral photoresponse from a two-terminal metal-oxide-semiconductor (MOS)-type detector with a capping layer of nc-Si-embedded mesoporous silica<sup>12</sup> (MS) and the enhancement is attributed to the transistorlike operation of the device, in which the inversion layer acts as the emitter while trapping of positive charges in the mesoporous dielectric layer assists the carrier injection from the inversion layer to the contact, resulting in current amplification.

The device structure is depicted schematically in Fig. 1. First, a 220-nm-thick MS template layer is formed on *p*-type Si substrates. Si nanocrystals were thereafter synthesized in the MS templates by using a plasma deposition process.<sup>12</sup> The size and crystalline nature of these embedded Si nanocrystals are revealed in the inset of Fig. 1 by a high-resolution image of cross-sectional transmission electron microscopy (TEM). One can see that the density of Si

nanocrystals in the MS film was in the order of  $2 \times 10^{18} \text{ cm}^{-3}$ . The average size of nc-Si was found to be  $\sim 4 \text{ nm}$ . For applying bias, a back Al contact layer and a top (transparent) indium tin oxide (ITO) electrode of  $2 \times 2.5 \text{ mm}^2$  are formed.

The photoluminescence (PL) spectra of the nanostructured films shown in Fig. 1 exhibit a broadband peak at 2.7 eV ( $\lambda=460 \text{ nm}$ ). Similar PL spectra were also observed from the germanium nanocrystals (nc-Ge)-embedded samples, as well as the reference sample of a pure MS template<sup>12</sup> but with a much lower intensity, indicating that the emission was weakly linked to the embedded nanocrystal structures. Hence, we attribute the observed blue PL emission to the interfacial states associated with neutral defects of oxygen vacancy<sup>13</sup> ( $\equiv\text{Si}-\text{Si}\equiv$ ) in the MS matrix. The embedded semiconductor nanocrystals, e.g., nc-Si, in the silica layer play a role by sensitizing the emission through generating more photoexcited carriers. These carriers are then trapped in the interfacial oxygen defects and subsequently

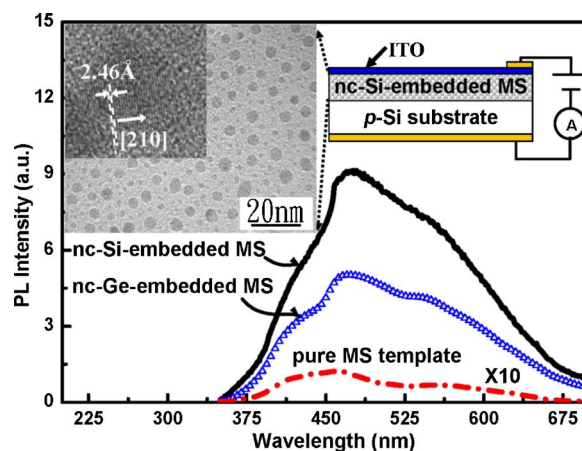


FIG. 1. (Color online) PL spectra of MS films embedded with Si or Ge nanocrystals, as well as the pure MS template, together with a schematic drawing illustrating the configuration of the ITO/nc-Si-embedded MS/*p*-Si photodetectors. The inset shows cross-sectional TEM images of the MS films with high density of silicon nanocrystals.

<sup>a)</sup>Electronic mail: jmsieh@mail.ndl.org.tw

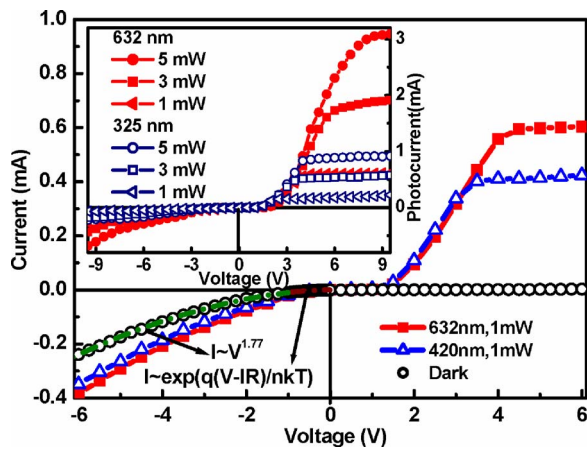


FIG. 2. (Color online) Current-voltage characteristics of ITO/nc-Si-embedded MS/*p*-Si devices in the dark and illuminated by 420 and 632 nm light of 1 mW. The inset is a plot of photocurrents for the same device irradiated with 325 and 632 nm light of 1, 3, and 5 mW, respectively, in which the photocurrents mean the measured current values after subtraction of the dark current.

recombine for an intense 460 nm PL emission. A shoulder peak also appeared in the spectra around 550–575 nm, which could be due to the band-to-band transition of Si nanocrystals with double-bonded oxygen atoms.<sup>14</sup>

Figure 2 shows current-voltage (*I*-*V*) characteristics of the device without illumination. A rectifying ratio of 87 was measured at  $\pm 3$  V. In the range of low forward bias from 0 to  $-0.9$  V, the *I*-*V* characteristic was fitted fairly using the equation given in Ref. 15 and presented in Fig. 2 by series connection of a diode (ideality factor  $\approx 2.1$ ) and a resistor (75 k $\Omega$ ). Over this range, a bias dependence of  $\sim V^{1.77}$  was obtained, indicating that space-charge-limited current dominates *I*-*V* characteristics.<sup>16</sup> Weak photoresponse was observed over a wide range of forward bias voltages (0 to  $-6$  V) when the device was irradiated with 420 and 632 nm light of 1 mW, respectively (Fig. 2).

Very different *I*-*V* characteristics were observed at reverse bias. As shown in Fig. 2, for the bias  $> 1.5$  V the originally very low reverse current (hereafter referred to as the dark current) increased drastically when the device was illuminated with light in the wavelength range of 300–700 nm (only several typical curves are depicted here). The increase of photocurrent exhibited a linear dependence with increase of voltage at lower reverse bias until the current saturated to a value  $I_S$  at higher bias. Note that  $I_S$  increases with the incident light power at a given wavelength, while it is higher for incident light of the same power but at longer wavelengths (see the inset of Fig. 2).

Figure 3 summarizes the measured photoresponse over a wide range of incident light wavelengths for the ITO/nc-Si-embedded MS/*p*-Si MOS detectors at bias voltages of  $\pm 5$  V, together with a reference curve obtained for the same device structure but without a capping layer, namely, ITO/*p*-Si diodes. The photoresponse values plotted in the figure were calculated after subtracting the dark current at the corresponding bias. Biased at +5 V, the photoresponse of an ITO/*p*-Si structure increased essentially linearly with wavelength from 300 to 700 nm by three times. The ITO/nc-Si-embedded MS/*p*-Si detector showed essentially the same spectral response for both forward and reverse biases, except for the two peaks observed at 425 and 580 nm. Significantly,

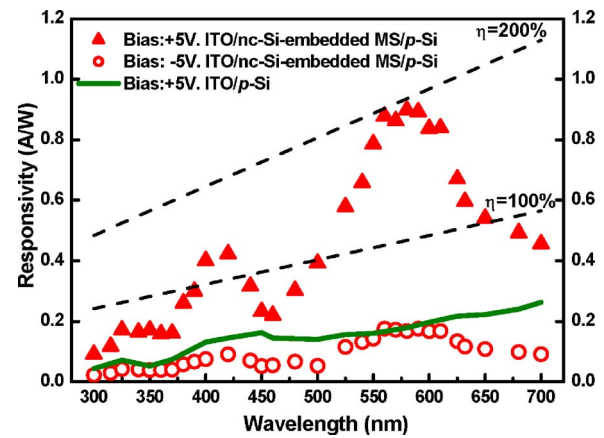


FIG. 3. (Color online) Spectral dependence of the photoresponse of detectors with ITO/nc-Si-embedded MS/*p*-Si and ITO/*p*-Si structures.

much more enhanced photoresponse (a factor of 4–5) was measured at reverse bias, which were as high as 0.4 and 0.9 A/W at the above two wavelengths, respectively.

For convenience, two guidelines were plotted in Fig. 3, representing the quantum efficiency ( $\eta$ ) values of 100% and 200%, respectively. For two spectral ranges, i.e., 375–475 and 500–650 nm, we measured conversion efficiency values of more than 100% and as high as nearly 200% at 580 nm for the ITO/nc-Si-embedded MS/*p*-Si detector. Therefore, there must be an amplification mechanism to enhance the measured photoresponse at reverse bias. Furthermore, it is noted that the enhancement factor between forward and reverse cases is independent of illumination intensity if dark current is subtracted (see the inset of Fig. 2). Low dark currents with high dynamic resistance of 1.3 M $\Omega$  and high photoresponse yield high detectivity of  $\sim (1-2) \times 10^{12}$  cm Hz<sup>0.5</sup> W<sup>-1</sup> for the present detector.<sup>17</sup>

The measured response time of the detector was around 10 ns presumably constrained by nonradiative lifetime (2.5 ns) as previously reported in mesoporous siliceous materials.<sup>18</sup> This value is much faster than those demonstrated by photoconductive detectors.<sup>5,8</sup> Hence, photoconductive gain was ruled out as a major mechanism in the enhancement of reverse photocurrents of our ITO/nc-Si-embedded MS/*p*-Si detectors.<sup>5,8,19</sup>

Based on the above experimental evidence, we propose the following mechanism to explain why the detector efficiency could be more than 100% through this two-terminal detector with a nc-Si-embedded MS layer as the absorption medium. This is illustrated in Fig. 4. Before illumination, the device operates like a normal MOS capacitor, i.e., a significant number of electrons are accumulated at the MS-Si interface forming a *n*-type inversion layer if a large enough reverse bias is applied. Only a few carriers could flow over the MS barrier layer, leading to a considerably low dark current. Upon optical excitation, strong absorption occurs for incident photons with the energies matching the transition energies from the ground hole states ( $E_h^0$ ) to the ground electron states ( $E_e^0$ ) (the gap energy between the highest occupied molecular orbital and the lowest unoccupied molecular orbital according to Ref 14), and the ground hole states ( $E_h^0$ ) to the excited states ( $E_e^*$ ) in connection to the Si-O interface states as well. With the applied electric field, the excited electrons in the  $E_e^0$  and  $E_e^*$  states are driven towards the ITO contact layer via the tunneling process. The holes, however,



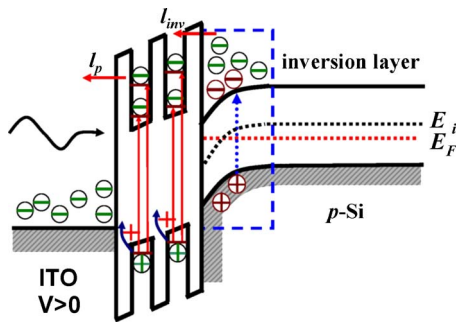


FIG. 4. (Color online) Illustration of transistorlike operation of an ITO/nc-Si-embedded MS/*p*-Si device under reverse bias and illumination. The symbols  $I_p$  and  $I_{inv}$  in the figure represent photoexcited and injected currents, respectively.

will be trapped by the interface states<sup>20</sup> with the energy level somewhat above the ground hole state ( $E_h^0$ ). The immobile positive charge centers will subsequently lower the barrier height, causing the resonant injection of electrons from the inversion layer through the MS layer to the ITO contact. Therefore, the measured photocurrent is expected to be composed of two parts, i.e., the photoexcited electrons plus the injected electrons. The mechanism of current amplification observed in this work is thus similar to that of a conventional phototransistor.<sup>10</sup> In particular, the enhancement of photoresponsivity measured at 425 and 580 nm, respectively, can be explained by the two resonant states of the nc-Si/MS system.<sup>4,14,20</sup>

The situation is different when the gate bias is changed from positive to negative. Although excited electrons in this case are expected to move to the side of the Si substrate, recombination with holes in the surface accumulation layer will significantly reduce the charge transport. At the same time, there will be little enhancement of hole transport from the MS layer to ITO, since the photogenerated holes are mostly trapped at the interface states. Therefore, the measured current would not differ too much from the case without photoexcitation.

In summary, we demonstrated efficient ITO/nc-Si-embedded MS/*p*-Si MOS detectors with enhanced photoreponse from UV to visible light. The enhancement effect was explained by the transistorlike operation mechanism when the device was operated at reverse bias. The primary photo-

current generated in the nc-Si of the MS layer was amplified due to the electron injection from the inversion layer through the MS dielectric to the ITO contact. Therefore, the measured optoelectronic conversion efficiency can be as high as 200%.

The authors acknowledge the financial support by the National Science Council of Taiwan (NSCT) through various grants including PPAEU-II and the ATU program of the Ministry of Education, Taiwan, R.O.C.

- <sup>1</sup>P. Yu, J. Topolancik, and P. Bhattacharya, *IEEE J. Quantum Electron.* **40**, 1417 (2004).
- <sup>2</sup>H. Ouyang, C. C. Striemer, and P. M. Fauchet, *Appl. Phys. Lett.* **88**, 163108 (2006).
- <sup>3</sup>F. Gan, L. Hou, G. Wang, H. Liu, and J. Li, *Mater. Sci. Eng., B* **76**, 63 (2000).
- <sup>4</sup>M. V. Wolkin, J. Jorne, P. M. Fauchet, G. Allan, and C. Delerue, *Phys. Rev. Lett.* **82**, 197 (1999).
- <sup>5</sup>O. M. Nayfeh, S. Rao, A. Smith, J. Therrien, and M. H. Nayfeh, *IEEE Photonics Technol. Lett.* **16**, 1927 (2004).
- <sup>6</sup>J. P. Zheng, K. L. Jiao, W. P. Shen, W. A. Anderson, and H. S. Kwok, *Appl. Phys. Lett.* **61**, 459 (1992).
- <sup>7</sup>M. K. Lee, C. H. Chu, Y. H. Wang, and S. M. Sze, *Opt. Lett.* **26**, 160 (2001).
- <sup>8</sup>S. M. Sze, *Physics of Semiconductor Devices*, 2nd ed. (Wiley, New York, 1981), Chap. 13, pp. 743–770.
- <sup>9</sup>R. McClintock, A. Yasan, K. Minder, P. Kung, and M. Razeghi, *Appl. Phys. Lett.* **87**, 241123 (2005).
- <sup>10</sup>A. Elfving, M. Larsson, G. V. Hansson, P.-O. Holtz, and W.-X. Ni, *Mater. Res. Soc. Symp. Proc.* **770**, I2.2 (2003).
- <sup>11</sup>A. Elfving, A. Karim, G. V. Hansson, and W.-X. Ni, *Appl. Phys. Lett.* **89**, 083510 (2006).
- <sup>12</sup>A. T. Cho, J. M. Shieh, J. Shieh, Y. F. Lai, B. T. Dai, F. M. Pan, H. C. Ku, Y. C. Lin, K. J. Chao, and P. H. Liu, *Electrochem. Solid-State Lett.* **8**, G143 (2005).
- <sup>13</sup>J. Y. Zhang, X. M. Bao, Y. H. Ye, and X. L. Tan, *Appl. Phys. Lett.* **73**, 1790 (1998).
- <sup>14</sup>A. Puzder, A. J. Williamson, J. C. Grossman, and G. Galli, *Phys. Rev. Lett.* **88**, 097401 (2002).
- <sup>15</sup>T. A. Burr, A. A. Seraphin, E. Werwa, and K. D. Kolenbrander, *Phys. Rev. B* **56**, 4818 (1997).
- <sup>16</sup>M. A. Rafiq, Y. Tsuchiya, H. Mizuta, S. Oda, Shigeyasu Uno, Z. A. K. Durrani, and W. I. Milne, *Appl. Phys. Lett.* **87**, 182101 (2005).
- <sup>17</sup>C. K. Wang, T. K. Ko, C. S. Chang, S. J. Chang, Y. K. Su, T. C. Wen, C. H. Kuo, and Y. Z. Chiou, *IEEE Photonics Technol. Lett.* **17**, 2161 (2005).
- <sup>18</sup>Y. L. Liu, W. Z. Lee, J. L. Shen, Y. C. Lee, P. W. Cheng, and C. F. Cheng, *Appl. Phys. Lett.* **85**, 6350 (2004).
- <sup>19</sup>S. K. Zhang, W. B. Wang, I. Shtau, F. Yun, L. He, H. Morkoc, X. Zhou, M. Tamargo, and R. R. Alfano, *Appl. Phys. Lett.* **81**, 4862 (2002).
- <sup>20</sup>S. H. Choi and R. G. Elliman, *Appl. Phys. Lett.* **74**, 3987 (1999).